arXiv:1302.0367v1 [cond-mat.mtrl-sci] 2 Feb 2013

Order of Decay of Mobile Charge Carriers in P3HT:PCBM Solar Cells

Carsten Deibel,[1, a] Daniel Rauh,[2] and Alexander Foertig[1]
[1]*Experimental Physics VI, Julius-Maximilians-University of Würzburg, 97074 Würzburg, Germany*
[2]*Bavarian Center for Applied Energy Research e.V. (ZAE Bayern), D-97074 Würzburg, Germany*

(Dated: February 5, 2013)

The charge carrier dynamics of organic solar cells are directly related to the loss mechanisms limiting the photovoltaic performance. In this study we derive and determine the recombination order Δ of the mobile fraction of charge carriers, as it directly relevant to understand nongeminate losses of photocurrent. We compare it to the commonly reported order of decay for all charge carriers, δ, which is often determined from transient measurements. For annealed P3HT:PCBM solar cells, we find that δ is consistent with recombination of mobile with trapped charge carriers in tail states with a characteristic energy of about 40 meV, in analogy to previous studies. Furthermore, due to exposure of the devices to synthetic air for 30 h in the dark and, subsequently, 30 h under illumination, δ increases strongly while Δ decreases very slightly. The tail state energy rises to about 100 meV for 30 h oxygen exposure under illumination, implying that the tails become increasingly deeper, leading to more trapped charge carriers. The impact on the photocurrent, however, can be more easily judged by the recombination order Δ, which decreases only weakly from 1.70 to 1.62, i.e. a slight shift towards trap-assisted recombination. Finally, we show an approach to reconstruct the time dependence of the photoinduced charge carrier density from 10 µs to 100 ms, based on charge extraction and open circuit voltage decay measurements. We confirm this reconstruction by comparison to transient absorption data, and show that the resulting charge carrier dynamics are consistent with the order of decay δ. We discuss the interpretation of the recombination orders as figures of merit for charge carrier losses.

I. INTRODUCTION

The optimisation of organic solar cells is crucial for the successful commercialisation of these devices. Therefore, understanding the dominant loss mechanisms is an important task. In organic semiconductors with their low dielectric constant, Coulomb interactions are strong and can potentially hamper photogeneration—essentially by geminate recombination—and increase nongeminate recombination of charge carriers. Nevertheless, photogeneration in many state-of-the-art polymer–fullerene solar cells was found to be uncritical,[1–4] so that the dominant loss mechanism in state-of-the-art organic solar cells is usually nongeminate recombination. The latter is often observed as power law decay of the effective charge carrier concentration n_{eff} with time t, $n_{\mathrm{eff}}(t) \propto t^{-(\delta-1)}$, using transient absorption[5,6] and charge extraction techniques.[7–14] Such charge carrier dynamics correspond to loss currents j_{loss} and recombination rates R with high orders of decay δ,

$$j_{loss} \propto R \propto n^{\delta}. \qquad (1)$$

We point out that here and in the following, we dropped the subscript to denote an effective charge carrier density, and believe that the difference between effective density and electron density is clear from the context. The experimentally determined δ usually exceeds the value of two expected for recombination of electrons n and holes p in a homogeneous system without trapping, $R \propto np \propto n^2$. This is possible if the concentrations of electrons and holes available for recombination are imbalanced, for instance by doping or trapping. Trapping of charge carriers is invariably found in disordered systems such as the organic semiconductor blends described here.[15,16] For P3HT:PCBM solar cells, the dominant recombination mechanism was recently interpreted as recombination between mobile charge carriers and charge carriers trapped in an approximately exponential density of tail states.[12,13,17,18]

However, the photocurrent of a solar cell is only due to transport of the mobile fraction of the excess charge carriers.[19,20] Therefore, in order to judge the impact of loss mechanisms on the photocurrent, it is instructive to define the order of decay Δ of the density of *mobile* charge carriers n_c. Then,

$$j_{loss} \propto n_c^{\Delta}. \qquad (2)$$

For band–band recombination in a homogeneous system, $\Delta = 2$ is expected, whereas for trap-assisted recombination, $\Delta \to 1$.

With this paper, we offer a derivation of the recombination order for free charge carriers, Δ. We propose a connection between this figure of merit and the order of decay δ. For annealed P3HT:PCBM solar cells exposed to oxygen in dark and under illumination, we determine both δ and Δ to compare them. Finally, we consider the role of these recombination orders for characterising the loss mechanisms in organic solar cells.

II. EXPERIMENTAL

The investigated solar cells were prepared as follows: a 40 nm thick layer of poly(3,4-ethylenedioxythiophene):poly(styrenesulfonate) (CLEVIOS PVP AI4083) was spincoated on top of indium tin oxide/glass substrates. The substrates were transferred into a nitrogen glovebox. The coated substrates were heated to 130°C for 10 min to remove residual water. The $L = 190$ nm thick active layer consisting of poly(3-hexylthiophene-2,5-diyl) (P3HT):[6,6]-phenyl-C_{61} butyric acid methyl ester (PCBM)

---

[a] deibel@physik.uni-wuerzburg.de; deibel@disorderedmatter.eu

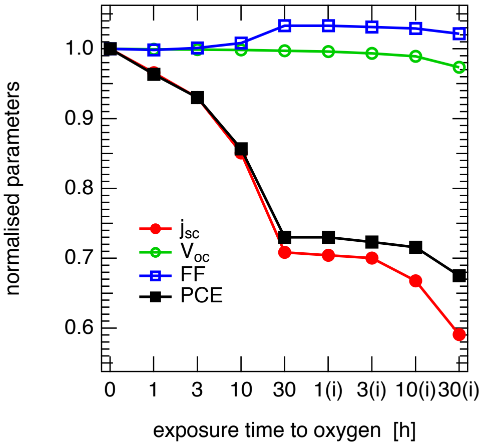

FIG. 1. Solar cell parameters normalised to the values of the fresh P3HT:PCBM solar cells. The loss of *PCE* upon oxygen exposure is mainly due to loss of short circuit current, whereas open circuit voltage and fill factor remain almost constant.

blend using a weight ratio of 1:0.8 was spin coated from chlorobenzene solution and thermally annealed at 130°C for 10 min subsequently. As cathode a Ca (3 nm)/Al (90 nm) electrode was thermally evaporated, with an active area of about 9 mm^2.

After current–voltage (IV) characterisation (Keithley 2602) under AM1.5g simulated illumination the samples were directly transferred to a Janis CCS 550 He contact gas cryostate, being exposed to ambient air for a few minutes. During the measurements the devices were stored in He atmosphere, during the degradation steps the cryostate was filled with synthetic air (80 % N_2, 20 % O_2, no moisture). The illumination was provided by a high power light emitting diode (LED) with 10 W electrical power (Seoul P7 Emitter). The calibration of the LED illumination level was performed using a silicon solar cell with a linear response of the short circuit current on the incident light intensity.

Charge extraction measurements were performed using the LED and a double pulse generator (Agilent 81150A) for applying the premeasured open circuit voltage V_{oc} to the solar cell. At a certain time defined as t_0, the LED was switched off by shorting the constant current source (Keithley 2602) with a high power transistor triggered by the double pulse generator. The resulting current was preamplified by a FEMTO DHPCA-100 current–voltage amplifier and recorded by an Agilent DSO 90254A oscilloscope. The time integration of the current was corrected for charges stored on the plates (electrodes), yielding the desired charge carrier densities. For the V_{oc} transients, a voltage amplifier with 1.5 GΩ input resistance was attached to the oscilloscope.

The measurement cycle was as follows: the light intensity was varied from 0.001 to 3.98 suns; at each illumination level an IV-curve as well as a charge extraction measurement was performed. Additionally, a V_{oc}-transient was recorded for an initial illumination level of 1.58 suns. The measurements were done before starting the degradation, after 1, 3, 10 and 30 h in dark. Afterwards the degradation under 1 sun illumination was started and the cell was characterized again after 1, 3, 10 and 30 h.

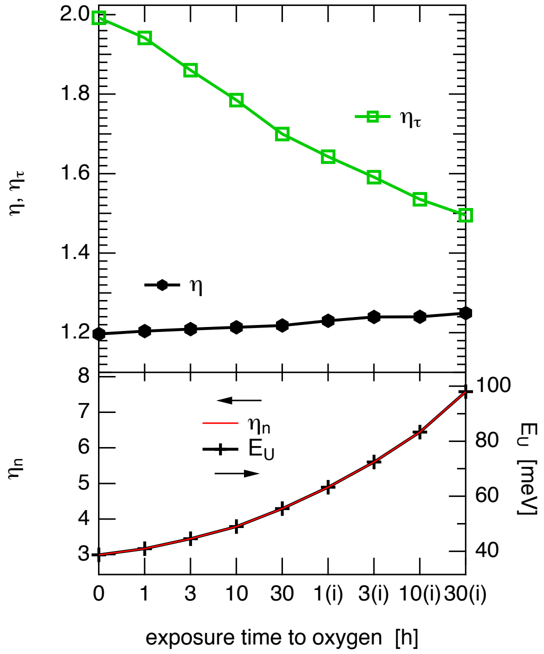

FIG. 2. Change of the diode ideality factor η and the ideality factors for the charge carrier concentration η_n (charge extraction data and Eqn. (4)) and lifetime η_τ (Eqn. (6)). The Urbach tail energy E_U, calculated from η_n by Eqn. (9), strongly increases with oxygen exposure time.

III. EXPERIMENTAL RESULTS

A. Steady-State Measurements

The P3HT:PCBM device used for this study showed solar cell parameters of open circuit voltage $V_{oc} = 0.57$ V, short circuit current density $j_{sc} = 8.2$ mA/cm^2, fill factor $FF = 69$ %, yielding a power conversion efficiency $PCE = 3.2$ % under AM1.5g illumination using a solar simulator. For dark oxygen exposure only j_{sc} dropped strongly by about 30 %, whereas V_{oc} remained constant and the fill factor increased by 3 %. For the additional oxygen exposure under illumination j_{sc} continued to decrease to about 60 % of its initial value, FF decreased back to 100 % and V_{oc} to 97 % of their initial values after additional 30 h under illumination, respectively (Fig. 1). The changes in the solar cell parameters upon oxygen exposure are consistent with Ref. 21, although there they decreased more quickly, which is probably due to the low UV emission of the LED used in the present study.

We consider the diode ideality factor η for providing insight into the dominant recombination mechanism.[17,22] It can be extracted from the Shockley diode equation under illumi-

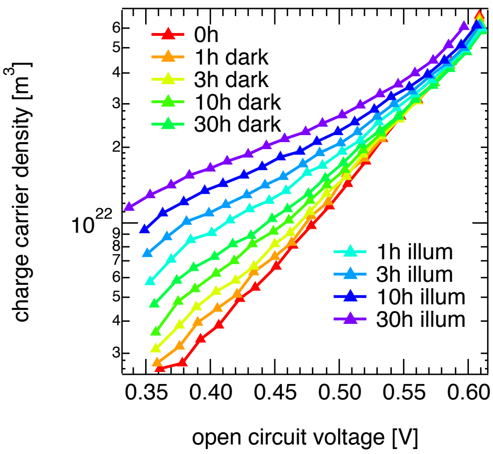

FIG. 3. The charge carrier density at open circuit conditions as obtained from charge extraction measurements for every degradation step.

nation, as

$$\eta = \left(\frac{kT}{q}\right)^{-1} \frac{dV_{oc}}{d\ln(j_{sc})}, \tag{3}$$

if the photogeneration is field independent. q is the elementary charge, kT the thermal energy, We determined η in the range from 0.001 to 0.4 suns. As shown in Fig. 2 (top), η increases continuously with oxygen exposure time from an initial value of 1.20 to 1.22 after 30 h of dark degradation and to 1.25 after the additional 30 h exposure under illumination.

The charge carrier density n from charge extraction measurements at open circuit conditions is shown in Fig. 3. For the nonexposed device, n shows the typical exponential dependence on V_{oc},[17,18]

$$n = n_0 \exp\left(\frac{qV_{oc}}{\eta_n kT}\right), \tag{4}$$

where n_0 is the dark carrier concentration and η_n the ideality factor for the carrier concentration.[18] The extracted charge carrier concentration n can be defined as the sum of mobile and shallowly trapped electrons and holes. Here and in the following, we assume that deeply trapped charge carriers, which cannot be extracted, do not play a major role in the recombination process. η_n signifies the voltage dependence of n as defined in Eqn. (4) and rises strongly with oxygen exposure time (Fig. 2 (bottom)). For mobile charge carriers, $\eta_n = 2$ would be expected, as their concentration is proportional to $\exp(qV/2kT)$ (c.f. Eqn. (4)).[17]

Recently, we introduced an approach connecting the diode ideality factor η with the ideality factors η_n and η_τ for charge carrier concentration and lifetime, respectively.[18] The latter is determined by the voltage dependence of τ,

$$\tau \propto \exp\left(-\frac{qV_{oc}}{\eta_\tau kT}\right). \tag{5}$$

By using[18]

$$\eta^{-1} = \eta_n^{-1} + \eta_\tau^{-1}, \tag{6}$$

we are able to calculate η_τ from the experimentally determined η and η_n. Ideally, a value of η_τ of 2 is expected,[23] and this is indeed the case for the fresh device. Recently it was shown that $\eta_\tau < 2$ can be due to inhomogeneous spatial charge carrier distributions in the device,[24] but clearly in our thick device it is rather homogeneous. However, we see in Fig. 2 (top) that η_τ decreases notably upon oxygen exposure down to about 1.5 for 30 h illumination, which is briefly discussed at the end of the next section.

In the following, our aim is to investigate the nongeminate loss mechanism in P3HT:PCBM solar cells.

B. Recombination Mechanism and Order of Decay

The nongeminate recombination rate R is empirically characterised by the order of decay δ, c.f. Eqn. (1). For a recombination with the same initial density of electrons and holes, $n \approx p$, a recombination order δ of approx. 2 is expected in homogeneous systems without trapping: Then, a pure Langevin recombination with $R \propto np = n^2$ would be observed.

However, charge transport in the disordered polymer–fullerene solar cells is based on hopping between localised states, and within the framework of multiple-trapping-and-release, tail states are expected to be prominent and have been observed experimentally by defect spectroscopy.[15,21,25–27] Therefore, in systems with trapping the overall electron (hole) concentration n (p) is given as the sum of mobile n_c (p_c) and immobile, trapped charge carriers n_t (p_t). However, under these conditions not all charge carriers are available for recombination at a given time, i.e., only the mobile ones can actively move to their oppositely charged recombination partners. In a homogeneous system, the recombination rate becomes

$$R \propto n_c p_c + n_c p_t + n_t p_c \propto np - n_t p_t \ll np, \tag{7}$$

as usually $n_c \ll n_t$, $p_c \ll p_t$. Here we have neglected that these contributions to recombination may have different prefactors. The immobile charge carriers cannot recombine with one another, therefore lowering the recombination rate and increasing the order of decay δ as the loss of the overall charge carrier concentration is reduced.

As shown recently for annealed P3HT:PCBM solar cells at room temperature, the recombination of mobile with shallow trapped charge carriers is dominant.[12,17,18,28] The contributions of electrons and holes cannot be directly distinguished, therefore we write for simplification

$$R \propto n_c(n_c + n_t) \approx n_c n_t. \tag{8}$$

For charge carriers trapped in exponential (Urbach) tails of the density of states distribution, n_t, the voltage dependence is weaker than for mobile charge carriers. Accordingly, $\eta_n > 2$. Indeed, the characteristic energy E_U can be directly calculated from η_n by[18]

$$E_U = \eta_n \frac{kT}{2}. \tag{9}$$

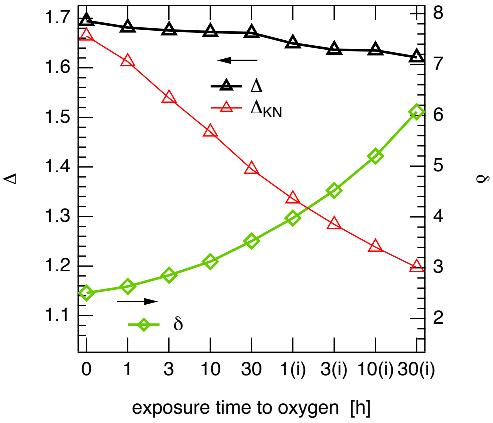

FIG. 4. The recombination order δ of all charge carriers (Eqn. (10)) is consistent with longer charge carrier lifetimes and more trapping due to deeper tail states. Considering only the free charge carriers, the recombination order Δ (Eqn. (2))—1 for first order, 2 for second order recombination—decreases slightly with oxygen exposure time. The recombination order for free charge carriers Δ_{KN} as defined in Ref. 24 overestimates this trend.

Therefore, E_U strongly increases with oxygen exposure time from the initial 40 meV—consistent with literature[17,28]—to about 100 meV, as shown in Fig. 2 (bottom). We point out that (a) exponential tails are only approximations of the density of states distribution for charge carriers, as discussed in more detail in Refs. 18 and 28, and (b) that we cannot distinguish between electrons and holes with charge extraction measurements. Using defect spectroscopy, we determined a somewhat higher characteristic tail state energy of 57 meV for an annealed P3HT–PCBM blend.[18]

The corresponding recombination order—defined by Eqn. (1)—can be calculated as[18]

$$\delta = \frac{\eta_n}{\eta_\tau} + 1. \tag{10}$$

Eqn. (10) allows to obtain information on the decay dynamics of the charge carrier concentration. The result is shown in Fig. 4: δ increases strongly with oxygen exposure time, to which η_n contributes about $3/4$ and η_τ only to about $1/4$. Clearly, $\delta > 2$, which implies that charge carrier doping or trapping are involved, and that the overall concentration n of free and shallow trapped charge carriers decays more slowly with time.

Concerning the nonideal value of η_τ, a possible reason for a value smaller than two is that the charge carrier mobility, to which the recombination prefactor is proportional, does depend on the voltage[29,30] (see Appendix B). However, η_τ also decreases upon increasing asymmetries between the electron and hole concentrations, e.g. by doping.[24]

C. Recombination Order of Free Charge Carriers

As recently pointed out by Kirchartz and Nelson,[24] a recombination order referring only to the mobile charge carriers n_c is a relevant figure of merit, as the (photo)current is due to the transport of free, mobile charge carriers.[20,31] Δ is defined by Eqn. (2) and was given by the authors as $(\delta-1)^{-1}+1$. Within our framework, we get a somewhat different result,

$$R \propto n_c^{\frac{2}{\eta}}, \tag{11}$$

which is derived in the Appendix A. The recombination order of mobile charge carriers, $\Delta = 2/\eta$, is interesting as it allows to interpret the diode ideality factor η directly in terms of the dominant recombination mechanism. Therefore, a value of $\Delta = 1$ corresponds to a first order charge carrier decay, for instance due to recombination exclusively through recombination centers. In constrast, $\Delta = 2$ implies that all charge carriers are free, so that they can recombine with one another in a second order decay as no trapping occurs. We point out that due to our definition, also the recombination orders between one and two are well defined.

In Fig. 4, we assembled the resulting orders of decay for all and for mobile charge carriers, δ and Δ, respectively. While δ increases strongly upon oxygen exposure, as discussed above, the order of decay for mobile charge carriers decreases from 1.70 to 1.62 slightly towards more trap-assisted recombination. In contrast, Δ_{KN} calculated according to Kirchartz and Nelson[24] decreases more strongly, potentially leading to an overestimation of the importance of first order recombination.

Thus, for trap-assisted recombination, $\Delta \to 1$, whereas $\delta > 2$ as outlined above. In a homogeneous system without doping or trapping, i.e. only mobile charge carriers, both δ and Δ become two as all charge carriers can contribute to recombination.

D. Charge Carrier Dynamics from Transient Measurements

We performed measurements of the open circuit voltage decay after switching the illumination with 1.58 sun intensity off, as shown in Fig. 5 (top). We point out that the open circuit voltage transients are similar for all degradation steps up to $5 \cdot 10^{-4}$ s, corresponding to the steady-state V_{oc} value at 0.001 suns illumination, whereas for later times the decay is slower for the solar cells longer exposed to oxygen. From the open circuit voltage transients (Fig. 2 (top)) η_τ was determined as described in the following. The derivative of the open circuit voltage decay with respect to $\ln t$ yields

$$\frac{dV_{oc}}{d\ln t} = \underbrace{\frac{dV_{oc}}{d\ln\tau}}_{-\eta_\tau \frac{kT}{q}} \underbrace{\frac{d\ln\tau}{d\ln t}}_{1}. \tag{12}$$

Here, $dV_{oc}/d\ln\tau$ is equal to $-\eta_\tau kT/q$ (c.f. Eqn. (5)), and the derivative $d\ln\tau/d\ln t$ yields unity as shown in Appendix C. Therefore, our intermediate result is that $dV_{oc}/d\ln\tau = dV_{oc}/d\ln t$. Thus, we were able to determine η_τ directly by fitting the open circuit voltage decay data for $t > 800$ μs. We point out that the resulting values are about $10-15$ % lower compared to η_τ calculated by Eqn. (6). A possible reason for

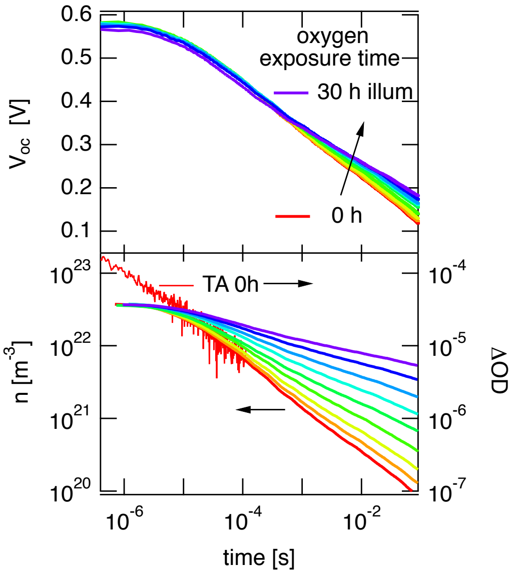

FIG. 5. (Top) V_{oc} transients after switching off the LED (1.58 sun), for each oxygen exposure step. The decays coincide until about $5 \cdot 10^{-4}$ s, corresponding to the steady-state value at 0.001 suns. At longer times, oxygen exposure decreases the slope of the carrier concentration decay. (Bottom) Calculated time evolution of the charge carrier density under open circuit conditions after switching the illumination off, as described in the text, illustrating the increasing recombination order upon oxygen exposure. For comparison, the optical density of photoinduced polaron absorption, determined by transient absorption (TA) at 980 nm probe wavelength, is shown.

this discrepancy is that the slope of the V_{oc} transients is not constant, leading to lower η_τ values at longer times.

Now, we have the means to consider the connection between transient and steady-state data,

$$\underbrace{\frac{dV_{oc}}{d\ln t}}_{-\eta_\tau \frac{kT}{q}} = \underbrace{\frac{dV_{oc}}{d\ln n}}_{\eta_n \frac{kT}{q}} \underbrace{\frac{d\ln n}{d\ln t}}_{-\frac{1}{\delta-1}} . \tag{13}$$

The term on the left hand side can be calculated according to Eqn. (12), the first term on the right hand side by Eqn. 4 and the second as shown in Appendix C. Equation (13) yields $(\delta - 1) = \eta_n/\eta_\tau$ and is, thus, consistent with Eqn. (10). We verified the behaviour of τ and η_τ by transient photovoltage measurements for oxygen exposed samples in the dark up to 30 h, finding similar results (not shown).

We are able to reconstruct the charge carrier dynamics $n(t)$ from the open circuit voltage transients and the ideality factors determined above. Thus, we mapped the $n(V_{oc})$ (Fig. 3) on the $V_{oc}(t)$ data (Fig. 5 (top)) to yield $n(V_{oc}(t)) = n(t)$ transients under open circuit conditions. The results in dependence on the oxygen exposure time are shown in Fig. 5 (bottom). The optical density of an unexposed P3HT:PCBM thin film, determined by transient absorption at 980 nm probe wavelength, is shown for comparison: the nongeminate recombination already starts at 10 ns (not shown) and reaches the upper µs range before vanishing in the noise level. Both data sets, transient absorption and reconstructed charge carrier dynamics, agree very well: The slope of the transient absorption data is the same as for the corresponding reconstructed charge carrier dynamics, although the latter shows the dynamics on a longer time scale up to 0.1 s. However, the reconstructed $n(t)$ data shown here cannot represent the time scales faster than 10 µs, because the $V_{oc}(t)$ data is not measured upon a laser pulse, but starts from a steady state illumination which is then switched off. Also, we point out that a major difference between transient absorption and open circuit voltage decays is that in the former, the photoinduced of the hole polaron on the polymer is measured, whereas $V_{oc}(t)$ yields the decay of excess charge carriers of both polarities. Therefore, asymmetries in photoinduced electron and hole concentrations would lead to different decays in transient absorption and the reconstruction shown here.

The resulting charge carrier transients, Fig. 5 (bottom), clearly show the impact of increasingly deeper tail states due to oxygen exposure: a slower decay, which is also seen in the open circuit voltage transients (Fig. 5 (top)), but is more pronounced for the reconstructed charge carrier dynamics. This slower nongeminate recombination is consistent with the strongly increasing order of decay δ (Fig. 4), as well as with previous experimental observations.[11,14,32,33] The slight decrease of the order of decay for free charge carriers Δ (Fig. 4), however, has a higher relevance to judge the impact of nongeminate recombination due to oxygen exposure on the photocurrent. This will be discussed in the next section.

IV. BRIEF COMMENT ON DOMINANT LOSS MECHANISM UPON OXYGEN EXPOSURE

Our focus within this manuscript was on establishing the connection between the orders of decay for all and mobile charge carriers as well as the reconstruction of the charge carrier dynamics from $V_{oc}(t)$ and $n(V_{oc})$ data. Nevertheless, as we considered annealed P3HT:PCBM solar cells exposed to oxygen exposure without and with illumination, we deem it appropriate to at least briefly comment on the origin of the performance losses shown in Fig. 1. The small decrease of the order of decay for *mobile* charge carriers corresponds to a slight shift towards more trap-assisted recombination. If we estimate the nongeminate losses from the light intensity dependent short circuit current,[34] we find that they remain at roughly 5 % for all degrees of exposure (not shown). We point out that this evaluation requires the assumption of recombination order of 2, and can therefore only serve as rough estimate. Nevertheless, the fill factor also remains almost constant upon oxygen exposure, which is unexpected for any carrier concentration or voltage dependent loss mechanism such as nongeminate recombination or field dependent photogeneration, respectively. Similarly, the decreasing short circuit current density does not even partially recover to its maximum value even at -3.5 V reverse bias (not shown), as would be expected for the combination of doping and nongeminate recombination as major losses. A field dependent process, either field dependent photogeneration or the development of an s-shape,[35] is only seen for the sample exposed to oxygen for 30 h under illumination. Therefore, in terms of absolute losses we tend to believe that the major effect for the degradation conditions considered is the (voltage independent) loss of photoexcitations,[36,37] not absorption,[38] in accordance with Refs. 39–41.

Nevertheless, while not the dominant loss mechanism under the conditions considered here, nongeminate recombination of charge carriers does change upon oxygen exposure, and may become more critical for exposure times longer than the range studied here: the increasingly deeper tail states, partly interpreted as doping in the literature,[21,40] are connected to an increase in the recombination order. At the same time, the charge carrier mobility was shown to be reduced by about 20 % for the time range considered here.[21]

V. CONCLUSIONS

We derived the recombination order of the mobile fraction of charge carriers, Δ, and find it to be twice the inverse diode ideality factor. This figure of merit is relevant for evaluating the dominant nongeminate losses of photocurrent. We compared Δ to the order of decay for all charge carriers, δ. For annealed P3HT:PCBM solar cells exposed to oxygen, partly under illumination, we found that δ increases strongly. We confirm this finding by a combination of charge extraction and open circuit voltage decay measurements, allowing us to reconstruct the charge carrier dynamics. In analogy to previous studies, we conclude that the dominant nongeminate loss mechanism is recombination of mobile and trapped charge carriers, the latter residing in approximately exponential tail states. The corresponding tail state energy rises from about 40 meV to 100 meV for 30 h oxygen exposure under illumination, implying that the fraction of trapped charge carriers increases. In contrast to δ, the recombination order of mobile charge carriers Δ is reduced weakly from 1.70 to 1.62 due to oxygen exposure, which implies a slight shift towards trap-assisted recombination. Thus, while δ provices a very sensitive measure of changes in the nongeminate recombination process, Δ is a useful figure of merit to directly determine the recombination order relevant to the photocurrent from the diode ideality factor.

ACKNOWLEDGMENTS

The authors thank Vladimir Dyakonov, Alexander Wagenpfahl, Andreas Baumann and Jens Lorrmann for interesting discussions, and Clemens Grünewald for providing the transient absorption data. The current work was supported by the Deutsche Forschungsgemeinschaft within the PHORCE project (Contract No. DE 830/8-1). C.D. gratefully acknowledges the support of the Bavarian Academy of Sciences and Humanities.

Appendix A: Recombination order for free charge carriers

Kirchartz and Nelson[24] showed the simple but useful connection between the high order recombination δ obtained from transient experiments to the recombination order of free charge carriers, Δ. Assuming a recombination rate of the form of Eqn. (8), i.e.

$$R \propto n_c n_t \propto n^{\delta} \tag{A1}$$

with

$$n_t \propto n_c^{\frac{kT}{E_U}} \tag{A2}$$

and $(\delta - 1) \approx \frac{E_U}{kT}$, the authors found

$$R \propto n_c^{\frac{1}{\delta-1}+1} \propto n_c^{\Delta}. \tag{A3}$$

Thus, the recombination order for free charge carriers was given as

$$\Delta_{KN} = (\delta - 1)^{-1} + 1. \tag{A4}$$

Within our framework, we consider the same recombination mechanism,

$$R = k' n_c n \approx k' n_c n_t \tag{A5}$$

for $n_c \ll n_t \approx n$, which is assumed by Kirchartz and Nelson as well. We write

$$R \propto n^{\delta} \approx n_t^{\delta} = n_c^{\frac{2}{\eta_n}\delta}. \tag{A6}$$

with $n_t \propto n_c^{\frac{2}{\eta_n}}$,[18] which is equivalent to Eqn. (A2). Using Eqns. (6) and (10), we get $\eta = \eta_n/\delta$ and therefore

$$R \propto n_c^{\frac{2}{\eta_n}\left(\frac{\eta_n}{\eta_\tau}+1\right)} = n_c^{2(\eta_\tau^{-1}+\eta_n^{-1})} = n_c^{\frac{2}{\eta}} \equiv n_c^{\Delta}. \tag{A7}$$

Thus, $\Delta = 2/\eta$, c.f. Eqn. (11). This is equivalent to Eqn. (A4) only in the case of $\eta_\tau = 2$.

The connection between Δ and δ follows from the comparison of Eqns. (A6) and (A7): $\Delta = \frac{2}{\eta_n}\delta$.

Appendix B: Impact of the recombination prefactor on η_τ

Considerung the effective recombination rate $R = n/\tau$ allowed to derive the ideality factor η_n and η_τ and their relation to the diode ideality factor, c.f. Eqn. (6).[18] Comparing it to the recombination rate for mobile–trapped recombination, Eqn. (A5), the effective lifetime becomes

$$\tau = \frac{1}{k' n_c} \tag{B1}$$

for this recombination mechanism. Considering the contribution of the voltage dependencies $k'(V) \propto \exp(qV/\eta_\mu kT)$ and

$n_c \propto \exp(qV/2kT)$, we find in analogy to the derivation in Ref. 18 that

$$\eta_\tau^{-1} = \eta_\mu^{-1} + 2^{-1}. \tag{B2}$$

Assuming that the effective lifetime is indeed proportional to the inverse mobile carrier concentration with factor $1/2$ in the exponent, it follows for the voltage dependence of the mobility that

$$\eta_\mu = \frac{1}{\eta_\tau^{-1} - \frac{1}{2}}. \tag{B3}$$

For the fresh device, $\eta_\tau = 2$, therefore $\eta_\mu \to \infty$: a field independent mobility in the voltage range considered here. However, for the device exposed to oxygen under illumination, $\eta_\tau = 1.5$, yielding $\eta_\mu = 6$. Considering that the internal field points in the opposite direction than the external voltage V, this value implies a mobility with a negative field dependence. This is possible, as shown by simulations[29] and experiments.[30] However, a decreasing value of η_τ can also be due to an asymmetry of the electron and hole concentration, e.g. by doping.[24]

Appendix C: Connection of τ and t

Considering the recombination rate $R = n/\tau$ in its empirical form together with Eqn. (A5), we can state $\tau = 1/(kn^{\delta-1})$. The derivative of $\ln\tau$ with respect to $d\ln t$, as referred to in Eqn. (12), is then given as

$$\begin{aligned}\frac{d\ln\tau}{d\ln t} &= -\frac{d\ln kn^{\delta-1}}{d\ln t}\\ &= -(\delta-1)\frac{d\ln kn}{d\ln t} = -(\delta-1)\left(-\frac{1}{\delta-1}\right) = 1. \end{aligned} \tag{C1}$$

Here, the $d\ln n/d\ln t$ yields $-1/(\delta-1)$, as $n(t) \propto t^{-\frac{1}{\delta-1}}$ is equivalent to Eqn. (A5).

Appendix D: Calculating the Effective Lifetime

With our approach, we can calculate the effective charge carrier lifetime from the reconstructed $n(t)$ data as

$$\tau(n) = \frac{n}{R(n)} = -\frac{n}{\frac{dn}{dt}}. \tag{D1}$$

Alternatively, τ can be determined directly from the open circuit voltage decay, according to

$$\frac{dV_{oc}}{dt} = \frac{kT}{q}\frac{\frac{dn}{dt}}{n} = -\eta_n \frac{kT}{q}\tau^{-1} \tag{D2}$$

$$\tau = -\eta_n \frac{kT}{q}\left(\frac{dV_{oc}}{dt}\right)^{-1}. \tag{D3}$$

Here, dn/dt was calculated by using Eqn. (4). Zaban et al.[42] already derived Eqn. (D3) a decade ago, but neglected to include η_n. Therefore, their Equation leads to an underestimation of the effective lifetime if $\eta_n > 1$, which is indeed the case for the data shown here (Fig. 2). Thus, generally, both open circuit voltage decay and $n(V_{oc})$ data is required for the calculation of the effective lifetime or the reconstruction of the charge carrier dynamics.

---

[1] R. A. Street, S. Cowan, and A. J. Heeger, Phys. Rev. B **82**, 121301(R) (2010).

[2] J. Kniepert, M. Schubert, J. C. Blakesley, and D. Neher, J. Phys. Chem. Lett. **2**, 700 (2011).

[3] M. Gluecker, A. Foertig, V. Dyakonov, and C. Deibel, Phys. Stat. Sol. (RRL) **6**, 337 (2012).

[4] A. A. Bakulin, A. Rao, V. G. Pavelyev, P. H. M. van Loosdrecht, M. S. Pshenichnikov, D. Niedzialek, J. Cornil, D. Beljonne, and R. H. Friend, Science **335**, 1340 (2012).

[5] I. Montanari, A. F. Nogueira, J. Nelson, J. R. Durrant, C. Winder, M. A. Loi, N. S. Sariciftci, and C. Brabec, Appl. Phys. Lett. **81**, 3001 (2002).

[6] T. Offermans, S. C. J. Meskers, and R. A. J. Janssen, J. Chem. Phys. **119**, 10924 (2003).

[7] C. G. Shuttle, B. O'Regan, A. M. Ballantyne, J. Nelson, D. D. C. Bradley, J. de Mello, and J. R. Durrant, Applied Physics Letters **92**, 093311 (2008).

[8] C. Deibel, A. Baumann, and V. Dyakonov, Appl. Phys. Lett. **93**, 163303 (2008).

[9] G. Juška, K. Genevičius, N. Nekrašas, G. Sliaužys, and G. Dennler, Appl. Phys. Lett. **93**, 143303 (2008).

[10] A. Foertig, A. Baumann, D. Rauh, V. Dyakonov, and C. Deibel, Appl. Phys. Lett. **95**, 052104 (2009).

[11] A. Baumann, T. J. Savenije, D. H. K. Murthy, M. Heeney, V. Dyakonov, and C. Deibel, Adv. Funct. Mater. **21**, 1687 (2011).

[12] R. A. Street, Phys. Rev. B **84**, 075208 (2011).

[13] R. C. I. MacKenzie, C. G. Shuttle, M. L. Chabinyc, and J. Nelson, Adv. Ener. Mater. **2**, 662 (2012).

[14] D. Rauh, C. Deibel, and V. Dyakonov, Adv. Funct. Mater. **22**, 3371 (2012).

[15] J. Schafferhans, A. Baumann, C. Deibel, and V. Dyakonov, Appl. Phys. Lett. **93**, 093303 (2008).

[16] R. A. Street, A. Krakaris, and S. R. Cowan, Adv. Funct. Mater. **22**, 4608 (2012).

[17] T. Kirchartz, B. E. Pieters, J. Kirkpatrick, U. Rau, and J. Nelson, Phys. Rev. B **83**, 115209 (2011).

[18] A. Foertig, J. Rauh, V. Dyakonov, and C. Deibel, Phys. Rev. B **86**, 115302 (2012).

[19] A. Rudenko and V. I. Arkhipov, Phil. Mag. B **45**, 177 (1982).

[20] S. D. Baranovskii, H. Cordes, F. Hensel, and G. Leising, Phys. Rev. B **62**, 7934 (2000).

[21] J. Schafferhans, A. Baumann, A. Wagenpfahl, C. Deibel, and V. Dyakonov, Org. Electron. **11**, 1693 (2010).

[22] W. Shockley and W. T. Read, Jr., Phys. Rev. **87**, 835 (1952).

[23] C. van Berkel, M. J. Powell, A. R. Franklin, and I. D. French, J. Appl. Phys. **73**, 5264 (1993).

[24] T. Kirchartz and J. Nelson, Phys. Rev. B **86**, 165201 (2012).

[25] M. Meier, S. Karg, K. Zuleeg, W. Brütting, and M. Schwoerer, J. Appl. Phys. **84**, 87 (1998).

[26] N. von Malm, J. Steiger, H. Heil, R. Schmechel, and H. von Seggern, J. Appl. Phys. **92**, 7564 (2002).

[27] K. Vandewal, W. D. Oosterbaan, S. Bertho, V. Vrindts, A. Gadisa, L. Lutsen, D. Vanderzande, and J. Manca, Appl. Phys. Lett. **95**, 123303 (2009).

[28] R. C. I. MacKenzie, T. Kirchartz, G. F. A. Dibb, and J. Nelson, J. Phys. Chem. C **115**, 9806 (2011).

[29] L. J. A. Koster, Phys. Rev. B **81**, 205318 (2010).

[30] S. Albrecht, W. Schindler, J. Kurpiers, J. Kniepert, J. C. Blakesley, I. Dumsch, S. Allard, K. Fostiropoulos, U. Scherf, and D. Neher, J. Phys. Chem. Lett. **3**, 640 (2012).

[31] D. Monroe, Phys. Rev. Lett. **54**, 146 (1985).

[32] J. Nelson, Phys. Rev. B **67**, 155209 (2003).

[33] C. G. Shuttle, N. D. Treat, J. D. Douglas, J. M. J. Fréchet, and M. L. Chabinyc, Adv. Ener. Mater. **2**, 111 (2012).

[34] L. J. A. Koster, M. M. Wienk, K. Maturová, and R. A. J. Janssen, Adv. Mater. **23**, 1670 (2011).

[35] A. Wagenpfahl, D. Rauh, M. Binder, C. Deibel, and V. Dyakonov, Phys. Rev. B **82**, 115306 (2010).

[36] A. Sperlich, H. Kraus, C. Deibel, H. Blok, J. Schmidt, and V. Dyakonov, J. Phys. Chem. B **115**, 13513 (2011).

[37] S. Cook, A. Furubea, and R. Katoh, J. Mater. Chem. **22**, 4282 (2012).

[38] A. Guerrero, P. P. Boix, L. F. Marchesi, T. Ripolles-Sanchis, E. C. Pereira, and G. Garcia-Belmonte, Sol. Energy Mat. Sol. Cells **100**, 185 (2012).

[39] M. O. Reese, A. M. Nardes, B. L. Rupert, R. E. Larsen, D. C. Olson, M. T. Lloyd, S. E. Shaheen, D. S. Ginley, G. Rumbles, and N. Kopidakis, Adv. Funct. Mater. **20**, 3476 (2011).

[40] H. Hintz, H. Peisert, H.-J. Egelhaaf, and T. Chasse, J. Phys. Chem. C **115**, 13373 (2011).

[41] F. Deschler, A. D. Sio, E. von Hauff, P. Kutka, H.-J. E. T. Sauermann, J. Hauch, and E. D. Como, Adv. Funct. Mater. **22**, 1461 (2012).

[42] A. Zaban, M. Greenshtein, and J. Bisquert, Chem. Phys. Chem. **4**, 859 (2003).